Angular Distribution of Characteristic Radiation Following the Excitation of He-Like Uranium in Relativistic Collisions

Alexandre Gumberidze, Daniel B. Thorn, Andrey Surzhykov, Christopher J. Fontes, Dariusz Banaś, Heinrich F. Beyer, Weidong Chen, Robert E. Grisenti, Siegbert Hagmann, Regina Hess, et al.

atoms

MDPI

Article

Angular Distribution of Characteristic Radiation Following the Excitation of He-Like Uranium in Relativistic Collisions

Alexandre Gumberidze [1,*], Daniel B. Thorn [2], Andrey Surzhykov [3,4,5], Christopher J. Fontes [6], Dariusz Banaś [7], Heinrich F. Beyer [8], Weidong Chen [9], Robert E. Grisenti [8,10], Siegbert Hagmann [8,10], Regina Hess [8], Pierre-Michel Hillenbrand [8,10], Paul Indelicato [11], Christophor Kozhuharov [8], Michael Lestinsky [8], Renate Märtin [8,12], Nikolaos Petridis [8], Roman V. Popov [13], Reinhold Schuch [14], Uwe Spillmann [8], Stanislav Tashenov [15], Sergiy Trotsenko [8,12], Andrzej Warczak [16], Günter Weber [8,12], Weiqiang Wen [17], Danyal F. A. Winters [8], Natalya Winters [8], Zhong Yin [18] and Thomas Stöhlker [8,12,19]

1 ExtreMe Matter Institute EMMI and Research Division, GSI Helmholtzzentrum für Schwerionenforschung, 64291 Darmstadt, Germany
2 Lawrence Livermore National Laboratory, Livermore, CA 94550-9234, USA; thorn3@llnl.gov
3 Physikalisch-Technische Bundesanstalt, D-38116 Braunschweig, Germany; andrey.surzhykov@ptb.de
4 Institut für Mathematische Physik, Technische Universität Braunschweig, D-38106 Braunschweig, Germany
5 Laboratory for Emerging Nanometrology Braunschweig, D-38106 Braunschweig, Germany
6 Los Alamos National Laboratory, Computational Physics Division, Los Alamos, NM 87545, USA; cjf@lanl.gov
7 Institute of Physics, Jan Kochanowski University, PL-25-406 Kielce, Poland; d.banas@ujk.edu.pl
8 GSI Helmholtzzentrum für Schwerionenforschung, 64291 Darmstadt, Germany; h.beyer@gsi.de (H.F.B.); grisenti@atom.uni-frankfurt.de (R.E.G.); S.Hagmann@gsi.de (S.H.); r.hess@gsi.de (R.H.); P.M.Hillenbrand@gsi.de (P.-M.H.); c.kozhuharov@gsi.de (C.K.); m.lestinsky@gsi.de (M.L.); r.maertin@hi-jena.gsi.de (R.M.); n.petridis@gsi.de (N.P.); u.spillmann@gsi.de (U.S.); s.trotsenko@gsi.de (S.T.); g.weber@hi-jena.gsi.de (G.W.); D.Winters@gsi.de (D.F.A.W.); n.winters@gsi.de (N.W.); t.stoehlker@hi-jena.gsi.de (T.S.)
9 Institute of High Energy Physics, Chinese Academy of Sciences, Dongguan 523803, China; chenwd@ihep.ac.cn
10 Institut für Kernphysik, Goethe-Universität Frankfurt, 60486 Frankfurt am Main, Germany
11 Laboratoire Kastler Brossel, Sorbonne Université, CNRS, ENS-PSL Research University, Collège de France, 4, place Jussieu, F-75005 Paris, France; paul.indelicato@lkb.upmc.fr
12 Helmholtz-Institut Jena, D-07743 Jena, Germany
13 Department of Physics, St. Petersburg State University, 198504 St. Petersburg, Russia; st016948@student.spbu.ru
14 Physics Department, Stockholm University, S-106 91 Stockholm, Sweden; schuch@fysik.su.se
15 Physikalisches Institut, Ruprecht-Karls-Universität Heidelberg, 69120 Heidelberg, Germany; tashenov@physi.uni-heidelberg.de
16 Institute of Physics, Jagiellonian University, 30-348 Krakow, Poland; WarczakA@netmail.if.uj.edu.pl
17 Institute of Modern Physics, Chinese Academy of Sciences, Lanzhou 730000, China; wenweiqiang@impcas.ac.cn
18 Laboratory for Physical Chemistry, ETH Zürich, 8093 Zürich, Switzerland; zhong.yin@phys.chem.ethz.ch
19 Institut für Optik und Quantenelektronik, Friedrich-Schiller-Universität Jena, 07743 Jena, Germany
* Correspondence: a.gumberidze@gsi.de

Abstract: In this paper, we present an experimental and theoretical study of excitation processes for the heaviest stable helium-like ion, that is, He-like uranium occurring in relativistic collisions with hydrogen and argon targets. In particular, we concentrate on angular distributions of the characteristic Kα radiation following the K $\rightarrow$ L excitation of He-like uranium. We pay special attention to the magnetic sub-level population of the excited $1s2l_j$ states, which is directly related to the angular distribution of the characteristic Kα radiation. We show that the experimental data can be well described by calculations taking into account the excitation by the target nucleus as well as by the target electrons. Moreover, we demonstrate for the first time an important influence of the electron-impact excitation process on the angular distributions of the Kα radiation produced by excitation of He-like uranium in collisions with different targets.

Citation: Gumberidze, A.; Thorn, D.B.; Surzhykov, A.; Fontes, C.J.; Banaś, D.; Beyer, H.F.; Chen, W.; Grisenti, R.E.; Hagmann, S.; Hess, R.; et al. Angular Distribution of Characteristic Radiation Following the Excitation of He-Like Uranium in Relativistic Collisions. *Atoms* **2021**, *9*, 20. https://doi.org/10.3390/atoms9020020

Academic Editor: Emmanouil P. Benis

Received: 5 February 2021
Accepted: 12 March 2021
Published: 25 March 2021

Keywords: highly-charged ions; X-rays; storage rings; relativistic collisions; excitation

1. Introduction

The excitation of an electron bound to an ion is one of the fundamental atomic processes taking place in ion-atom collisions. The excitation processes have been intensively studied for light [1–3] to medium heavy ions [4–9], whereas in the high-Z regime the experimental investigations have been relatively scarce. Heavy ion storage rings, such as the Experimental Storage Ring (ESR) at GSI Helmholtzzentrum für Schwerionenforschung in Darmstadt, equipped with internal gas targets provide very favorable conditions to extend the studies of the excitation processes into the high-Z regime. In a series of experiments, the K-shell excitation has been studied for very heavy hydrogen- and helium-like ions [10–12]. Namely, the excitation of projectile electrons due to the interaction with the target nucleus has been addressed in detail. In these studies, the emphasis was put on the K-shell excitation cross sections to different fine structure levels of the L-shell along with the angular distributions of the subsequent Lyman-α and Kα radiation which provides access to the magnetic sub-level populations of the different fine structure states. The experimental data were well described by fully relativistic calculations [13].

In [14,15], it has been shown that in relativistic collisions between a highly-charged ion and a light atom, resulting in the excitation of the ion, the target electrons and nucleus can be considered as acting independently in the collision process. This is mainly due to the fact that the momentum transfers in such collisions are much larger than the typical momenta of the atomic electrons. Consequently, the excitation of a heavy projectile in fast asymmetric collisions can be described as a sum of two independent processes; proton-(or nucleus-) impact excitation (PIE) and electron-impact excitation (EIE). Here, we would like to note that for these two processes the acronyms HEX and EEX are used in plasma physics. The cross sections for the two processes scale as Z_T^2 and Z_T, respectively (Z_T being the target atomic number) [14–17]. Therefore, the relative contribution of the two processes is different for different targets, for example, the relative contribution of EIE would be largest for a hydrogen target, whereas for heavy targets the excitation will be dominated by the contribution due to the target nucleus. This property can be exploited to experimentally access the EIE process for the heaviest H- and He-like ions. For such heavy few-electron ions, a direct study of EIE represents a significant challenge due to the need of first producing the heavy highly-charged ions in sufficient quantities and then colliding them with the electron beam of sufficient intensity and energy. Therefore, direct studies of the EIE process, mostly performed at Electron Beam Ion Trap (EBIT) facilities, have been limited to low- and mid-Z ions up to now [18–21].

Owing to the development of a new multi-phase target for the ESR [22,23] that provides densities of up to 10^{15} particles/cm^2, we were able to experimentally access for the first time the EIE for H- and He-like uranium [24,25]. Namely, by looking at the ratios of the characteristic transitions produced by the K-L excitation and the following decay, the contribution of the EIE process has been unambiguously identified when comparing the data for an H_2 target with those for heavier targets, that is, N_2 and Ar, which can be well described by the PIE calculations. The state-of-the-art calculations combining both PIE and EIE processes [13,15,26,27] have been found to be in good agreement with our experimental data regarding the excitation cross sections to different fine structure states. Moreover, the comparison between our experimental data and the theory clearly demonstrated the importance of including the generalized Breit interaction in the calculations of the EIE process for both H- and He-like uranium ions.

In [28], we have addressed angular differential cross sections for the Lyman-α_1 transition ($2p_{3/2} \rightarrow 1s_{1/2}$) produced by the excitation of H-like uranium in collisions with H_2 and N_2 targets. The angular distributions provide access to the characteristics of magnetic sub-level population for the $2p_{3/2}$ state and the corresponding alignment, serving as a

stringent test of the underlying theoretical approaches. In [28], it has been found that in contrast to the ratios of the characteristic line intensities, where EIE plays a prominent role for an H_2 target, the corresponding angular distributions are relatively insignificantly affected by the EIE process and thus its influence could not be identified experimentally taking into account the corresponding uncertainties.

In the current paper, we present an experimental and theoretical study of the angular distributions for the Kα radiation produced by K-shell excitation of He-like uranium in relativistic collisions with H_2 and Ar targets. This work is an extension of our previous studies for H- and He-like uranium [25,28]. In contrast to the case of H-like uranium [28], here we demonstrate for the first time a clear role of the EIE process in the angular distributions of the Kα radiation for the excitation of He-like uranium in collisions with different targets.

2. Experiment

The detailed description of the experimental setup used in this study can be found in [25]. Here, we just briefly summarize the most important aspects. A beam of 10^8 He-like uranium ions, produced by successive acceleration and stripping, was stored and cooled in the ESR storage ring. To induce and measure the excitation, the stored ion beam was overlapped with an internal gas-jet target of the ESR oriented perpendicuraly to the beam axis. The experiment was performed for H_2 and Ar targets at two different beam energies of 218 MeV/u and 300 MeV/u. The target area densities were between 10^{13} and 10^{14} particles/cm^2. The kinetic energies for equivelocity electrons in the rest frame of the ions corresponding to the ion beam energies of 218 MeV/u and 300 MeV/u are 119.6 keV and 164.8 keV, respectively, whereas the K-L excitation energies are in the range of 96–101 keV for He-like uranium. Thus, both energies are above the EIE threshold for this case. In order to gain access to the angular distribution of the projectile Kα radiation produced by the K-L excitation process and the following decay of the excited states, the beam-target interaction zone was observed by an array of Ge(i) detectors, covering observation angles in the range between 35° and 150° with respect to the beam axis. The X-ray detectors were energy and efficiency calibrated before the experiment using a set of appropriate radioactive sources. The quantum efficiencies of the X-ray detectors for the Kα X-rays of He-uranium were in the range of 70–100%. The solid angles covered by the detectors ($\Delta\Omega/4\pi$) were on the order of 10^{-3}.

3. Results and Discussion

3.1. Experimental Data and Evaluation

In Figure 1 we present, as an example, the X-ray spectrum for $U^{90+}\rightarrow H_2$ collisions at 218 MeV/u recorded at the observation angle of 35° with respect to the ion beam direction. In the spectrum, the characteristic Kα and Kβ lines produced by the K-shell excitation of He-like uranium and the subsequent decay are prominent. In addition, broad lines associated with the radiative electron capture (REC) of the target electron into the projectile L and M shells are clearly visible along with the Bremsstrahlung background.

In the following, we focus on the Kα lines to gain insight into the excitation process of He-like uranium. Here, Kα_1 and Kα_2 lines comprise $[1s_{1/2}, 2p_{3/2}]^1P_1, [1s_{1/2}, 2p_{3/2}]^3P_2 \rightarrow [1s^2]^1S_0$ and $[1s_{1/2}, 2p_{1/2}]^3P_1, [1s_{1/2}, 2s_{1/2}]^3S_1 \rightarrow [1s^2]^1S_0$ transitions (see Figure 2), respectively which cannot be resolved by our detectors. The number of counts recorded in the Kα_1 and Kα_2 spectral lines were obtained by fitting the corresponding peaks in the spectra with Gaussian functions on top of a linear background due to Bremsstrahlung. In addition, the number of counts in the Kα_1 and Kα_2 lines were corrected for the energy-dependent detector efficiency. For this correction, an error of 3% is included.

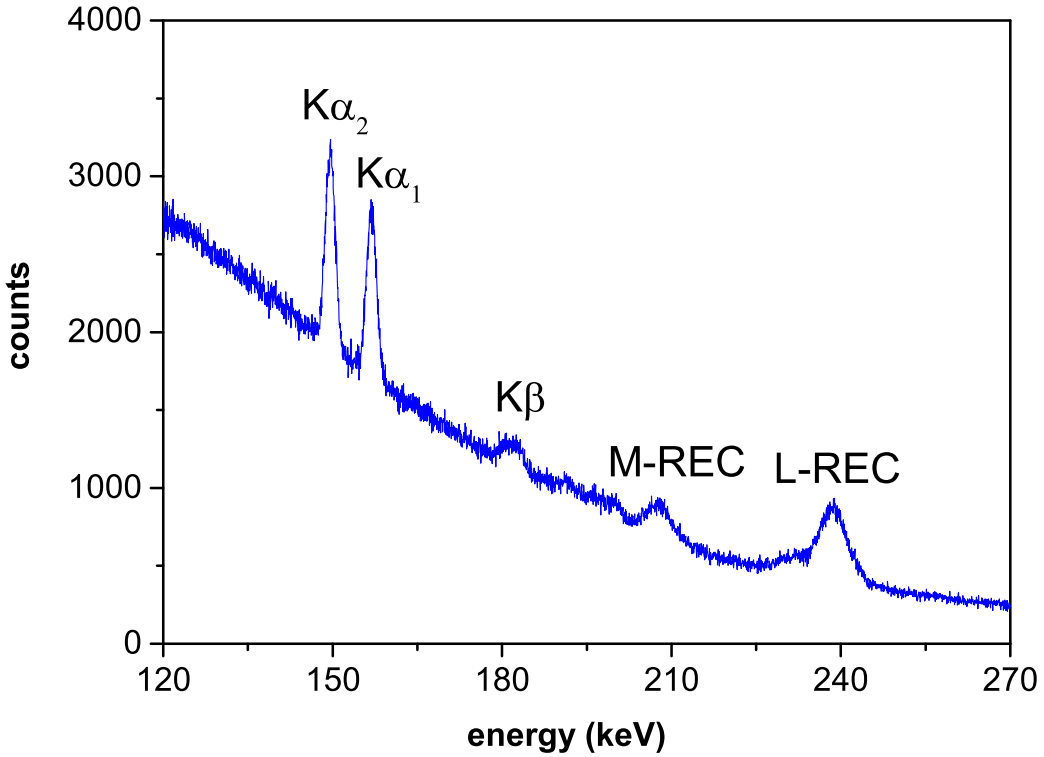

Figure 1. X-ray spectrum recorded for 218 MeV/u $U^{90+} \rightarrow H_2$ collisions with a Ge(i) detector at the observation angle of 35° with respect to the ion beam. The radiative electron capture (REC) transitions into L, M and higher shells are clearly visible together with the characteristic transitions into the K-shell.

Generally, in order to obtain the angular distribution of the Kα_1 and Kα_2 lines, one would have to correct their intensities for the different solid angles covered by the corresponding X-ray detectors. This correction introduces a significant uncertainty which can be avoided if one uses another transition with a known angular distribution for normalization. This method has been successfully used in our previous studies [12,28]. Nevertheless, for the current case, as already pointed out in our earlier works [12,25,28], it is not possible to obtain the angular distributions separately for the Kα_1 or Kα_2 lines, just by calculating their intensity ratio for different observation angles. This is due to the fact that in general both Kα_1 and Kα_2 lines can be anisotropic. This is in contrast to the case of H-like ions, where the ratio of Lyα_1 and Lyα_2 line intensities provides directly the angular distribution of the Lyα_1 transition in the ion frame due to the strict isotropy of the Lyα_2 transition [12,28]. In order to circumvent this problem, we use our older study where the angular distributions of the Kα_1 or Kα_2 lines have been measured for excitation of He-like uranium in collisions with an N_2 target at 217 MeV/u [12]. In this study, it was found that the measured angular distributions and the associated alignment parameters can be well described by calculations taking into account only the PIE process. This can be understood by considering the fact that for an N_2 target the relative contribution of EIE is suppressed by a factor of Z_T. Therefore, considering the fact that our current measurement has been carried out at basically the same collision energy, we can use the measured angular distributions from the older study [28] for our case of an Ar target at 218 MeV/u, where PIE should be prevalent as in the case of an N_2 target. Thus, in the following we consider the angular distribution of the Kα_1 line measured for $U^{90+} \rightarrow$ Ar collisions at 218 MeV/u to be known and we use it for normalization of other lines for both targets and both energies.

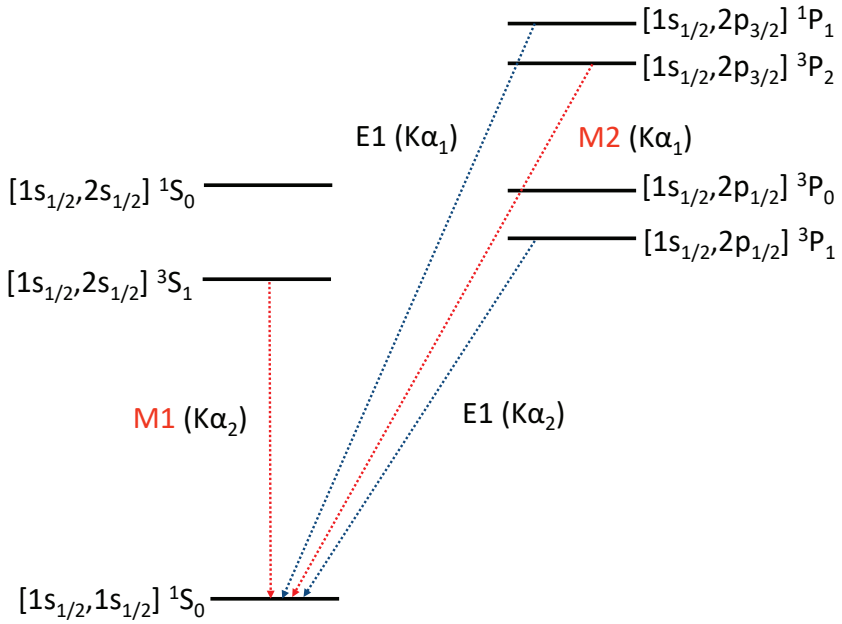

Figure 2. K- and L-shell levels of He-like uranium along with the transitions contributing to the observed Kα_1 and Kα_2 lines.

3.2. Theoretical Background

The angular distribution of the intensity of the Kα lines in He-like uranium can be generally described by the following formula [12,29];

$$W(\theta_{lab}) \propto \frac{1}{\gamma^2(1-\beta\cos\theta_{lab})^2}\left[1+\beta_2^{eff}\left(1-\frac{3}{2}\frac{\sin^2\theta_{lab}}{\gamma^2(1-\beta\cos\theta_{lab})^2}\right),\right] \quad (1)$$

where θ_{lab} is the photon observation angle with respect to the beam direction in the laboratory frame. β and γ are relativistic factors corresponding to the particular beam energy. Here, we would like to note that the factor in front of the square bracket which describes the relativistic solid angles transformation (between the emitter/projectile and laboratory frames) cancels out for the ratio of line intensities measured at the same beam energy. The angular emission patterns of the Kα spectral lines are determined by the effective anisotropy parameter β_2^{eff} which is in turn related to the alignment of the corresponding magnetic sub-levels whose exact form depends on the transition under consideration. Here, it has to be noted that for the excitation of He-like uranium, all four levels, $[1s_{1/2},2p_{3/2}]^1P_1$,$[1s_{1/2},2p_{3/2}]^3P_2$, $[1s_{1/2},2p_{1/2}]^3P_1$,$[1s_{1/2},2s_{1/2}]^3S_1$ can be in principle populated and thus contribute to the Kα_1 and Kα_2 lines. The $[1s_{1/2},2s_{1/2}]^1S_0$ and $[1s_{1/2},2p_{1/2}]^3P_0$ states decay via two-photon transitions and thus they do not contribute to the Kα_1 and Kα_2 lines. Therefore, the effective anisotropy parameter β_2^{eff} for the Kα_1 depends on the alignment parameters of the $[1s_{1/2},2p_{3/2}]^1P_1$ and $[1s_{1/2},2p_{3/2}]^3P_2$ states as well as on their (relative) populations and it is given by the following formula [29]:

$$\beta_2^{eff} = \frac{1}{\sqrt{2}}N(^1P_1)A_2(^1P_1) - \sqrt{\frac{5}{14}}N(^3P_2)A_2(^3P_2). \quad (2)$$

Here, $A_2(^1P_1)$ and $A_2(^3P_2)$ are alignment parameters of the $[1s_{1/2},2p_{3/2}]^1P_1$ and $[1s_{1/2},2p_{3/2}]^3P_2$ states, respectively, whereas $N(^1P_1)$ and $N(^3P_2)$ are their relative populations, with $N(^1P_1)+N(^3P_2)=1$.

Similarly, the effective anisotropy parameter β_2^{eff} for the Kα_2 is defined by the following formula:

$$\beta_2^{eff} = \frac{1}{\sqrt{2}} N(^3S_1) A_2(^3S_1) + \frac{1}{\sqrt{2}} N(^3P_1) A_2(^3P_1). \quad (3)$$

Here, $A_2(^3S_1)$ and $A_2(^3P_1)$ are alignment parameters of the $[1s_{1/2}, 2s_{1/2}]^3S_1$ and $[1s_{1/2}, 2p_{1/2}]^3P_1$ states, respectively, whereas $N(^3S_1)$ and $N(^3P_1)$ are their relative populations, with $N(^3S_1) + N(^3P_1) = 1$.

In order to obtain theoretical values for the alignment parameters, excitation cross sections to the corresponding magnetic sub-levels of the L-shell states for PIE and EIE processes are calculated. The PIE calculations are performed within fully relativistic framework where the electron-nucleus interaction is treated by the Liénard-Wiechert potential and (initial- and final-) states of helium-like ions are described by the multiconfiguration Dirac-Fock method. The EIE calculations are based on a relativistic distorted-wave approach [15,26,27] including the effects of the generalized Breit interaction.

In Tables 1 and 2, we present theoretical predictions for the alignment parameters A_2, the relative populations N, and the resulting effective anisotropy parameters β_2^{eff}, for case of hydrogen target, for all the states contributing to the Kα_1 and Kα_2 lines. The values are given separately for the case when only PIE process is taken into account as well as for the case where both PIE and EIE processes are included in the calculations. The theoretical values also include cascade contributions from excitation into higher levels.

Table 1. Theoretical values for the alignment parameters A_2, the relative populations N, and the resulting effective anisotropy parameters β_2^{eff} for $[1s_{1/2}, 2p_{3/2}]^1P_1$ and $[1s_{1/2}, 2p_{3/2}]^3P_2$ states contributing to the Kα_1 line. For details see text.

Beam Energy	Process	$A_2(^1P_1)$	$N(^1P_1)$	$A_2(^3P_2)$	$N(^3P_2)$	β_2^{eff}
218 MeV/u	PIE	−0.1694	0.9864	0.4473	0.0135	−0.1218
	PIE + EIE	−0.2161	0.7861	−0.3517	0.2138	−0.0751
300 MeV/u	PIE	−0.0359	0.9843	0.4969	0.01567	−0.0296
	PIE + EIE	−0.1367	0.8773	−0.2874	0.1226	−0.0637

Table 2. Theoretical values for the alignment parameters A_2, the relative populations N, and the resulting effective anisotropy parameters β_2^{eff} for $[1s_{1/2}, 2s_{1/2}]^3S_1$ and $[1s_{1/2}, 2p_{1/2}]^3P_1$ states contributing to the Kα_2 line. For details see text.

Beam Energy	Process	$A_2(^3S_1)$	$N(^3S_1)$	$A_2(^3P_1)$	$N(^3P_1)$	β_2^{eff}
218 MeV/u	PIE	0.1729	0.0442	0.1082	0.9557	0.0785
	PIE + EIE	0.0361	0.2555	−0.0731	0.7444	−0.0320
300 MeV/u	PIE	0.1352	0.0449	0.2279	0.9550	0.1582
	PIE + EIE	0.0658	0.1843	0.0227	0.8156	0.0217

3.3. Comparison with Theory

We obtain the experimental values for the effective anisotropy parameter β_2^{eff} by fitting Equation (1) to the angular distributions of the Kα_1 or Kα_2 lines observed in the experiment. For the fit, β_2^{eff} and the overall amplitude of the fit function were kept as free parameters.

Here, we would like to note that, in case of Kα_1, in general, Equation (1) has to be modified to account for an additional term proportional to the parameter β_4^{eff}. This additional term arises due to the decay of $^3P_2$ state, whose magnetic sub-level population is described by *two* alignment parameters, A_2 and A_4 [29]. However, our theoretical analysis has clearly shown that $\beta_4^{eff} << \beta_2^{eff}$ for all considered energies and targets. Moreover, we have confirmed this theoretical prediction by fitting our data (for Kα_1 line) with Equation (1)

including the additional term, which gives no significant difference (as compared to fitting with the unmodified version of Equation (1)) with respect to the obtained results for β_2^{eff}. Therefore, it is well justified to use Equation (1) for all cases in the current study.

In Table 3, we present our experimental results in comparison with the theoretical predictions for the effective anisotropy parameter for an argon target. The theoretical predictions include excitation only due to the interaction with the target nucleus (PIE), considering in addition the small screening effect due to the target electrons, but no EIE.

Table 3. Experimental values in comparison with theoretical predictions for the effective anisotropy parameters for the Kα_1 and Kα_2 lines of helium-like uranium ions produced by $K \rightarrow L$ excitation in collisions with argon atoms. PIE calculations were performed for the screened potential.

Beam Energy	Line	PIE Screened	Experiment
218 MeV/u	Kα_1	−0.1201	−0.12 ± 0.07 [12]
	Kα_2	0.0805	0.07 ± 0.02
300 MeV/u	Kα_1	−0.0273	0.02 ± 0.02
	Kα_2	0.1606	0.16 ± 0.03

As already mentioned above, for the argon target EIE is suppressed by a factor $Z_T = 18$ and thus this approximation is well justified. This has been also proven in our previous study for U^{90+}→N_2 collision at 217 MeV/u [12]. In addition to the direct excitation into L-shell, the theoretical predictions include cascade contributions from excitation into higher levels and following cascades leading to the population of the same L-shell levels. We would like to note that the cascade contributions to the effective anisotropy parameter are in all cases significantly smaller than the experimental uncertainties. From the comparison, a very good agreement between the experimental and theoretical results for the effective anisotropy parameter is obtained confirming the energy-dependence of the angular distributions addressed in our previous study [12]. Furthermore, the current experimental value for the effective anisotropy parameter of the Kα_2 line for $U^{90+}\rightarrow$ at 218 MeV/u agrees within the error bars with the value obtained in our previous measurement for the same line for U^{90+}→N_2 collision at 217 MeV/u [12]. This also serves as a consistency check for our method of using the angular distribution of Kα_1 line for $U^{90+}\rightarrow$ at 218 MeV/u as measured in the previous study [12] for normalization of other lines for both energies and targets.

In Table 4, we present a comparison between our experimental and theoretical values for the effective anisotropy parameter for Kα_1 and Kα_2 lines for an H_2 target at both energies.

Table 4. Experimental values in comparison with theoretical predictions for the effective anisotropy parameters for the Kα_1 and Kα_2 lines of helium-like uranium ions produced by $K \rightarrow L$ excitation in collisions with hydrogen molecules. For details see text.

Beam Energy	Line	PIE	PIE + EIE	Experiment
218 MeV/u	Kα_1	−0.1218	−0.0751	−0.11 ± 0.04
	Kα_2	0.0785	−0.0319	−0.07 ± 0.03
300 MeV/u	Kα_1	−0.0296	−0.0637	−0.02 ± 0.05
	Kα_2	0.1582	0.0217	0.04 ± 0.02

In this case, and in contrast to the Ar target, the theoretical predictions include, in addition to PIE, the EIE process as well. As already pointed out in our previous study, the EIE process plays a prominent role for the excitation of He-like uranium in collisions with H_2 [25]. As in the case of an Ar target, the theoretical values include cascade contributions from higher levels. Similarly to the case of Ar target, a good overall agreement between

the experimental and theoretical values can be stated. Furthermore, looking at the values in Table 4 we can conclude that for the Kα_1 line, the effect of the EIE on the effective anisotropy parameter is not significant, taking into account the corresponding experimental uncertainties. In other words, the experimental results agree both with predictions based on the PIE process only as well as with those where the EIE is included in addition to the PIE. The situation is very different for the Kα_2 line, where we see a clear influence of the EIE process which is also confirmed by the corresponding experimental values for both energies. The effect is more pronounced for 218 MeV/u where the EIE contribution leads to a change of sign for the effective anisotropy parameter for the Kα_2 line. This is also confirmed by comparison of the corresponding experimental results for Ar and H_2 targets (see Tables 3 and 4). In order to illustrate the effect of the EIE process on the effective anisotropy parameter, we present in Figure 3 angular distributions of the Kα_2 line intensity observed in our experiment for collisions of He-like uranium with Ar and H_2 targets at 218 MeV/u. The change in the shape of the angular distribution, corresponding to the changing sign of the effective anisotropy parameter, is evident. To the best of our knowledge, this is the first clear observation of the effect of EIE on the angular distributions of the subsequent characteristic transitions in heavy few-electron ions. Although previous experimental, as well as theoretical, studies of the excitation processes have revealed a clear dependence of the angular distribution on the collision energy [13,28], a dependence on the target could not be experimentally observed up to now [24,28].

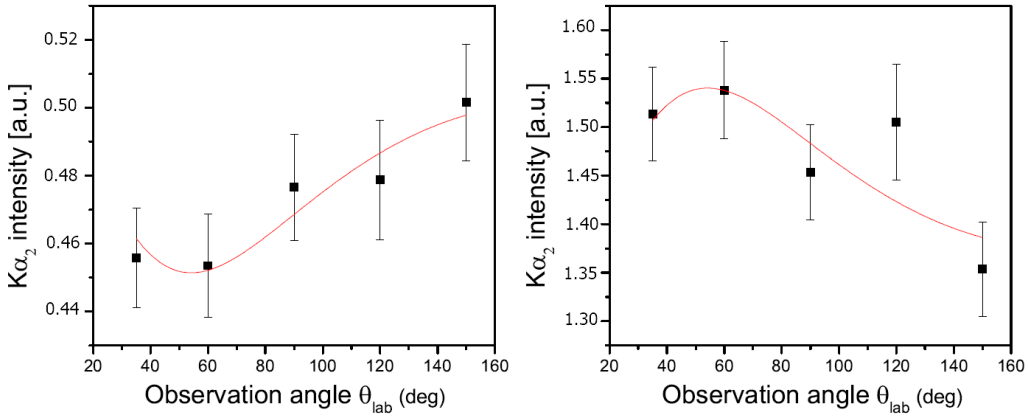

Figure 3. Angular distributions of Kα_2 line intensity measured for K-shell excitation of He-like uranium in collisions with argon (**left**) and hydrogen (**right**) targets at 218 MeV/u. In addition, fits of Equation (1) to the experimental data are shown by solid lines. The clear change of shape between the two targets is due to the contribution of the electron-impact excitation (EIE) process. For details see text.

When comparing the angular distribution and the corresponding effective anisotropy parameters for the Kα_2 line for the two targets, and thus looking at the effect of EIE on this observable, the following aspect should be taken into account. For an Ar target, where the projectile excitation is dominated by the PIE process, the Kα_2 spectral line contains almost exclusively the $[1s_{1/2}, 2p_{1/2}]^3P_1 \rightarrow [1s^2]^1S_0$ transition [25]. This is also clearly seen looking at the relative populations N (for PIE) in Table 2. For an H_2 target, where EIE plays an important role, excitation to the $[1s_{1/2}, 2s_{1/2}]^3S_1$ state becomes significant [25] (see also the corresponding relative populations N in Table 2) and thus the Kα_2 line in this case contains two transitions; $[1s_{1/2}, 2p_{1/2}]^3P_1, [1s_{1/2}, 2s_{1/2}]^3S_1 \rightarrow [1s^2]^1S_0$ which can not be resolved energetically by our semiconductor detectors. Therefore, a contribution of the EIE process to the angular distribution of the Kα_2 can be two-fold. Namely, the angular distribution might change due to the fact that the EIE process populates the magnetic sub-levels differently as compared to PIE, and thus the alignment of the $[1s_{1/2}, 2s_{1/2}]^3P_1$ state ($A_2(^3P_1)$) changes, or, the angular distribution could change because of an addition of

the $[1s_{1/2}, 2s_{1/2}]^3S_1 \rightarrow [1s^2]^1S_0$ transition to the Kα_2 line, due to the EIE process, without it changing the alignment of the $[1s_{1/2}, 2s_{1/2}]^3P_1$ state ($A_2(^3P_1)$). In order to shed more light on this aspect, we present, in Table 5, theoretical PIE and EIE cross sections for magnetic sub-levels of the $^3P_1$ state for 218 MeV/u.

Table 5. Partial cross sections for the excitation into magnetic sub-levels of the $^3P_1$ state for U^{90+} in collision with an H_2 target at 218 MeV/u. The results are given in barns.

	$m = 0$	$\|m\| = 1$
EIE	0.7898	0.5319
PIE	0.3423	0.4407

From the values in the table, we can conclude that the angular distribution of the Kα_2 line changes significantly not only due to an addition of the $[1s_{1/2}, 2s_{1/2}]^3S_1 \rightarrow [1s^2]^1S_0$ transition to this emission feature, but also due to the fact that the EIE process populates the magnetic sub-levels of the $[1s_{1/2}, 2s_{1/2}]^3P_1$ state very differently as compared to PIE, along with being more efficient than the latter in this collision energy range [30]. This is also reflected by the corresponding alignment values for the $^3P_1$ state as listed in Table 2.

4. Summary

In this work, we studied experimentally and theoretically the K-shell excitation of He-like uranium (U^{90+}) in collisions with Ar and H_2 targets at 218 and 300 MeV/u energies. In particular, we focused on angular distributions of the characteristic Kα_1 and Kα_2 lines induced by the K→L excitation process. State-of-the-art calculations which include both processes, PIE as well as EIE, provide a good agreement with the experimental data. Furthermore, by comparing the angular distributions and the corresponding effective anisotropy parameters for the two targets, we were able, for the first time, to clearly show an important role of the EIE process on the angular distribution of the Kα_2 line. This is in contrast to our previous studies for H- and He-like uranium [12,13,28] where only the role of PIE on the angular distributions was addressed, whereas the contribution of the EIE process to this observable could not be experimentally verified. Therefore, this work represents an important extension of our previous studies providing a deeper insight into the excitation processes and a sensitive test of the corresponding theories on the level of angular differential (and thus magnetic sub-level) cross sections.

Author Contributions: Conceptualization, A.G., D.B.T., A.S. and C.F.; Data curation, D.B.T.; Formal analysis, A.G., D.B.T. and R.V.P.; Funding acquisition, T.S.; Investigation, A.G., D.B.T., D.B., H.F.B., W.C., R.E.G., S.H., R.H., P.-M.H., P.I., C.K., M.L., R.M., N.P., R.S., U.S., S.T. (Stanislav Tashenov), S.T. (Sergiy Trotsenko), A.W., G.W., W.W., D.F.A.W., N.W., Z.Y. and T.S.; Methodology, A.S. and C.J.F.; Project administration, D.B.T.; Resources, R.E.G., N.P. and U.S.; Software, A.G. and D.B.T.; Supervision, A.G., D.B.T. and T.S.; Visualization, A.G.; Writing—original draft, A.G.; Writing—review and editing, A.S., C.J.F., P.-M.H., R.S. and T.S. All authors have read and agreed to the published version of the manuscript.

Funding: This research received no external funding.

Acknowledgments: This work was supported by the Helmholtz Alliance Program of the Helmholtz Association, contract HA216/EMMI "Extremes of Density and Temperature: Cosmic Matter in the Laboratory". The work of C.J. Fontes was supported by the U.S. Department of Energy through the Los Alamos National Laboratory, which is operated by Triad National Security, LLC, for the National Nuclear Security Administration of U.S. Department of Energy (Contract No. 89233218CNA000001). S.T. was supported by Deutsche Forschungsgemeinschaft (DFG), contract TA 740 1-1. This work was supported by SPbSU-DFG (Grants No. 11.65.41.2017 and No. STO 346/5-1). R.V.P. acknowledges also the financial support from the Foundation for the advancement of theoretical physics and mathematics "BASIS".

Conflicts of Interest: The authors declare no conflict of interest.

References

1. Detleffsen, D.; Anton, M.; Werner, A.; Schartner, K.H. Excitation of atomic hydrogen by protons and multiply charged ions at intermediate velocities. *J. Phys. B* **1994**, *27*, 4195. [CrossRef]
2. Reymann, K.; Schartner, K.H.; Sommer, B.; Träbert, E. Scaling relation for total excitation cross sections of He in collisions with highly charged ions. *Phys. Rev. A* **1988**, *38*, 2290. [CrossRef]
3. Anton, M.; Detleffsen, D.; Schartner, K.H.; Werner, A. Population of He 4^1D magnetic sublevels by collisions with protons and multiply charged ions in the intermediate velocity range. *J. Phys. B* **1993**, *26*, 2005. [CrossRef]
4. Stolterfoht, N. Zero-degree Auger spectroscopy in energetic, highly charged ion-atom collisions. *J. Electron Spectrosc. Relat. Phenom.* **1993**, *67*, 309. [CrossRef]
5. Stolterfoht, N.; Mattis, A.; Schneider, D.; Schiwietz, G.; Skogvall, B.; Sulik, B.; Ricz, S. Time-ordering effects in K-shell excitation of 170-MeV Ne^{7+} colliding with gas atoms: Double excitation. *Phys. Rev. A* **1995**, *51*, 350. [CrossRef] [PubMed]
6. Wohrer, K.; Chetioui, A.; Rozet, J.P.; Jolly, A.; Fernandez, F.; Stephan, C.; Brendle, B.; Gayet, R. Target nuclear charge dependence of 1s2 to 1s2p and 1s2 to 1s3p excitation cross sections of Fe24+ projectiles in the intermediate velocity range. *J. Phys. B* **1986**, *19*, 1997. [CrossRef]
7. Adoui, L.; Vernhet, D.; Wohrer, K.; Plante, J.; Chetioui, A.; Rozet, J.P.; Despiney, I.; Stephan, C.; Touati, A.; Ramillion, J.M.; et al. Excitation of Ar16+ projectiles in intermediate velocity collisions with neutrals. *Nucl. Instrum. Methods Phys. Res. Sect.* **1995**, *98*, 312. [CrossRef]
8. Vernhet, D.; Rozet, J.P.; Wohrer, K.; Adoui, L.; Stephan, C.; Cassimi, A.; Ramillion, J.M. Excitation in swift heavy ion-atom collisions. *Nucl. Instrum. Methods Phys. Res. Sect.* **1996**, *107*, 71. [CrossRef]
9. Brendle, B.; Gayet, R.; Rozet, J.P.; Wohrer, K. Application of the Schwinger Principle to Direct Excitation of Atoms or Ions by Impact of Bare Nuclei at Intermediate Velocities. *Phys. Rev. Lett.* **1985**, *54*, 2007. [CrossRef]
10. Stöhlker, T.; Ionescu, D.C.; Rymuza, P.; Bosch, F.; Geissel, H.; Kozhuharov, C.; Ludziejewski, T.; Mokler, P.H.; Scheidenberger, C.; Stachura, Z.; et al. K-shell excitation studied for H- and He-like bismuth ions in collisions with low-Z target atoms. *Phys. Rev. A* **1998**, *57*, 845. [CrossRef]
11. Gumberidze, A.; Fritzsche, S.; Bosch, F.; Ionescu, D.C.; Krämer, A.; Kozhuharov, C.; Stachura, Z.; Surzhykov, A.; Warczak, A.; Stöhlker, T. Shell- and subshell-resolved projectile excitation of hydrogenlike Au^{78+} ions in relativistic ion-atom collisions. *Phys. Rev. A* **2010**, *82*, 052712. [CrossRef]
12. Gumberidze, A.; Fritzsche, S.; Hagmann, S.; Kozhuharov, C.; Ma, X.; Steck, M.; Surzhykov, A.; Warczak, A.; Stöhlker, T. Magnetic-sublevel population and alignment for the excitation of H- and He-like uranium in relativistic collisions. *Phys. Rev. A* **2011**, *84*, 042710. [CrossRef]
13. Surzhykov, A.; Jentschura, U.D.; Stöhlker, T.; Gumberidze, A.; Fritzsche, S. Alignment of heavy few-electron ions following excitation by relativistic Coulomb collisions. *Phys. Rev. A* **2008**, *77*, 042722. [CrossRef]
14. Feinberg, B.; Gould, H.; Meyerhof, W.E.; Belkacem, A.; Hülskötter, H.-P.; Alonso, J.R.; Blumenfeld, L.; Dillard, E.; Guardala, N. Relativistic electron- and proton-impact ionization of highly stripped heavy ions determined from projectile-electron loss in H_2 and He. *Phys. Rev. A* **1993**, *47*, 2370. [CrossRef] [PubMed]
15. Najjari, B.; Voitkiv, A.B. Excitation of heavy hydrogenlike ions by light atoms in relativistic collisions with large momentum transfers. *Phys. Rev. A* **2012**, *85*, 052712. [CrossRef]
16. Zouros, T.J.M.; Lee, D.H.; Richard, P. Projectile 1s→2p excitation due to electron-electron interaction in collisions of O^{5+} and F^{6+} ions with H_2 and He targets. *Phys. Rev. Lett.* **1989**, *62*, 2261. [CrossRef] [PubMed]
17. Hülskötter, H.-P.; Meyerhof, W.E.; Gould, H.; Guardala, N. Evidence for Electron-Electron Interaction in Projectile JC-Shell Ionization. *Phys. Rev. Lett.* **1989**, *63*, 1938. [CrossRef]
18. Chantrenne, S.; Beiersdorfer, P.; Cauble, R.; Schneider, M.B. Measurement of electron impact excitation cross sections for heliumlike titanium. *Phys. Rev. Lett.* **1992**, *69*, 265. [CrossRef]
19. Wong, K.L.; Beiersdorfer, P.; Reed, K.J.; Vogel, D.A. Electron-impact excitation cross-section measurements of highly charged heliumlike and lithiumlike ions. *Phys. Rev. A* **1995**, *51*, 1214. [CrossRef]
20. Robbins, D.L.; Beiersdorfer, P.; Faenov, A.Y.; Pikuz, T.A.; Thorn, D.B.; Chen, H.; Reed, K.J.; Smith, A.J.; Boyce, K.R.; Brown, G.V.; et al. Polarization measurements of the Lyman-α_1 X-ray emission lines of hydrogenlike Ar^{17+} and Fe^{25+} at high electron-impact energies. *Phys. Rev. A* **2006**, *74*, 022713. [CrossRef]
21. Lindroth, E.; Orban, I.; Trotsenko, S.; Schuch, R. Electron-impact recombination and excitation rates for charge-state-selected highly charged Si ions. *Phys. Rev. A* **2020**, *101*, 062706. [CrossRef]
22. Kühnel, M.; Petridis, N.; Winters, D.F.A.; Popp, U.; Dörner, R.; Stöhlker, T.; Grisenti, R.E. Low- internal target from a cryogenically cooled liquid microjet source. *Nucl. Instrum. Meth. A* **2009**, *602*, 311. [CrossRef]
23. Petridis, N.; Kalinin, A.; Popp, U.; Gostishchev, V.; Litvinov, Y.A.; Dimopoulou, C.; Nolden, F.; Steck, M.; Kozhuharov, C.; Thorn, D.B.; et al. Energy loss and cooling of relativistic highly charged uranium ions interacting with an internal hydrogen droplet target beam. *Nucl. Instrum. Meth. A* **2011**, *656*, 1. [CrossRef]
24. Gumberidze, A.; Thorn, D.B.; Fontes, C.J.; Najjari, B.; Zhang, H.L.; Surzhykov, A.; Voitkiv, A.; Fritzsche, S.; Banas, D.; Beyer, H.; et al. Electron- and Proton-Impact Excitation of Hydrogenlike Uranium in Relativistic Collisions. *Phys. Rev. Lett.* **2013**, *110*, 213201. [CrossRef]

25. Gumberidze, A.; Thorn, D.B.; Surzhykov, A.; Fontes, C.J.; Najjari, B.; Voitkiv, A.; Fritzsche, S.; Banas, D.; Beyer, H.; Chen, W.; et al. Electron- and proton-impact excitation of helium-like uranium in relativistic collisions. *Phys. Rev. A* **2019**, *99*, 032706. [CrossRef]
26. Fontes, C.J.; Sampson, D.H.; Zhang, H.L. Inclusion of the generalized Breit interaction in excitation of highly charged ions by electron impact. *Phys. Rev. A* **1993**, *47*, 1009. [CrossRef]
27. Fontes, C.J.; Sampson, D.H.; Zhang, H.L. Use of the factorized form for the collision strength in exploration of the effect of the generalized Breit interaction. *Phys. Rev. A* **1994**, *49*, 3704. [CrossRef] [PubMed]
28. Gumberidze, A.; Thorn, D.B.; Fontes, C.J.; Najjari, B.; Zhang, H.L.; Surzhykov, A.; Voitkiv, A.; Fritzsche, S.; Banas, D.; Beyer, H.; et al. Ground-state excitation of heavy highly-charged ions. *J. Phys. B* **2015**, *48*, 144006. [CrossRef]
29. Surzhykov, A.; Jentschura, U.D.; Stöhlker, T.; Fritzsche, S. $K\alpha_1$ radiation from heavy, heliumlike ions produced in relativistic collisions. *Phys. Rev. A* **2006**, *74*, 052710. [CrossRef]
30. Najjari, B.; Voitkiv, A.B. Excitation of highly charged hydrogenlike ions by the impact of equivelocity electrons and protons: A comparative study. *Phys. Rev. A* **2013**, *87*, 034701. [CrossRef]